THE ASTROPHYSICAL JOURNAL, 293:83–93, 1985 June 1

MINKOWSKI'S OBJECT: A STARBURST TRIGGERED BY A RADIO JET

WIL VAN BREUGEL[1,2] AND ALEXEI V. FILIPPENKO[2,3]
Department of Astronomy, University of California, Berkeley
TIMOTHY HECKMAN[4,5]
Astronomy Program, University of Maryland; and Department of Physics and Astronomy, Johns Hopkins University
AND
GEORGE MILEY
Space Telescope Science Institute; and Leiden Observatory
Received 1984 October 18; accepted 1984 December 5

ABSTRACT

Radio and optical imaging, as well as optical spectrophotometry, are reported for "Minkowski's object," a peculiar blue object near the elliptical galaxy NGC 541 in the cluster Abell 194. The observations show that it is a region with bright optical line and continuum emission associated with a radio jet emanating from NGC 541. The radio and optical morphologies are similar to those of other extended emission-line regions associated with radio jets, such as in 3C 277.3. Optical emission is brightest near the edges of the jet, correlated with the absence of polarized radio emission, and filamentary downstream where the radio jet is deflected and decollimated. Moreover, gas velocities possibly increase downstream. These properties may be ascribed to the collision of a jet with relatively dense extranuclear gas. In Minkowski's object the origin of this gas could be related to its apparent location in a galactic bridge connecting NGC 541 with the nearby dumbbell system NGC 545/NGC 547.

There is a close resemblance between the line emission from Minkowski's object and that of both extragalactic H II regions and the prototypical starburst galaxy NGC 7714. Gas is therefore most likely photoionized by radiation from hot young stars. This interpretation is supported by comparisons with other possible excitation mechanisms, as well as by the presence of an unusually bright, blue continuum which probably exhibits Balmer absorption lines indicative of such stars. We conclude that Minkowski's object is an irregular galaxy currently undergoing a vigorous burst of star formation that was triggered by the radio jet.

Subject headings: galaxies: clustering — galaxies: individual — galaxies: jets — radio sources: galaxies — stars: formation

I. INTRODUCTION

In previous papers, we have discussed the properties of extended emission-line regions associated with radio jets and lobes in 3C 277.3 (Miley *et al.* 1981; van Breugel *et al.* 1985*a*, hereafter Paper I), 3C 305 (Heckman *et al.* 1982), 4C 26.42 (van Breugel, Heckman, and Miley 1984), 3C 293 (van Breugel *et al.* 1984), 3C 171 (Heckman, van Breugel, and Miley 1984), and 4C 29.30 (van Breugel *et al.* 1985*b*). A general conclusion from these observations and others reported for Centaurus A (Graham and Price 1981) and NGC 7385 (Hardee, Eilek, and Owen 1980; Simkin, Bicknell, and Bosma 1984) is that the optical emission-line regions form at the edges of radio jets which propagate through dense, inhomogeneous ambient media. When these jets collide with clouds, they can entrain (heat and accelerate) the gas and, as evidenced by the existence of blue stars near the outer jet in Cen A (e.g., Blanco *et al.* 1975), might even cause enhanced star formation along their trajectories (Osmer 1978; De Young 1981; Norman 1984).

Many of the related radio and optical properties in these objects may be explained in this manner. For example, the frequently distorted radio morphologies are thought to be caused by deflection and decollimation of the jets as they collide with clouds, and optical line emission is produced adjacent to bright radio emission through local ionization of the ambient gas. Moreover, the entrained ionized gas exhibits disturbed kinematics and depolarizes the radio emission.

In only a few cases is the optical line emission sufficiently bright to allow spectroscopic analysis of its excitation mechanism. Sometimes the spectra seem to indicate "in situ" power-law photoionization (e.g., 3C 277.3, Paper I) which is presumably related to the presence of the nearby jet. There is also evidence, however, that different ionization mechanisms may be dominant at different locations in Cen A (Phillips 1981; Brodie, Königl, and Bowyer 1983) and in 3C 277.3 (Paper I).

The study of radio/optical emission in jets is of interest because it may provide new constraints for hydrodynamic models of jets. These models predict well-developed interfaces between a jet and its ambient plasma (Norman *et al.* 1982; De Young 1984; Woodward 1984), precisely where most of the line-emitting gas is observed. As part of a survey to investigate the generality of such phenomena, we found a serendipitous radio source (PKS 0123−016A) whose jet is associated with the most spectacular emission-line region currently known in such objects.

PKS 0123−016A is a small head-tail radio source (O'Dea and Owen 1984) near the larger and more powerful radio

[1] Visiting Astronomer at the Very Large Array of the National Radio Astronomy Observatory, and at the European Southern Observatory.
[2] Visiting Astronomer at Lick Observatory.
[3] Miller Research Fellow.
[4] Visiting Astronomer at Kitt Peak National Observatory and Cerro Tololo Inter-American Observatory, of the National Optical Astronomy Observatories.
[5] Alfred P. Sloan Fellow.

TABLE 1

GLOBAL PROPERTIES OF OBJECTS

NGC 541	
Redshift	0.0181[a]
Luminosity distance	73 Mpc[b]
Linear/angular scale ratio	0.35 kpc arcsec^{-1}
Galaxy type	elliptical
Blue magnitude	13.0[a]
Minkowski's Object	
Redshift	0.0187
Distance from NGC 541	~18 kpc
Linear size	~4.5 × 5.5 kpc^2
Galaxy type	irregular
Blue magnitude	~17.5[c]
PKS 0123−016A	
Total flux density (1.4 GHz)	0.94 Jy[d]
Total power (1.4 GHz)	5.9 × 10^{30} ergs s^{-1} Hz^{-1}
Total luminosity (10^1–10^5 MHz)[d]	7.8 × 10^{40} ergs s^{-1}
Length of NE jet	~18 kpc
Flux density of nucleus (1.4 GHz)	~8.6 mJy
Power of nucleus (1.4 GHz)	5.3 × 10^{28} ergs s^{-1} Hz^{-1}
Position of nucleus[e]	$\alpha(1950) = 01^h23^m11^s.147 \pm 0^s.03$ $\delta(1950) = -01°38'21''.09 \pm 0''.3$

[a] Tonry and Davis 1981.
[b] $H_0 = 75$ km s^{-1} Mpc^{-1}.
[c] Simkin 1976.
[d] Andernach 1981.
[e] Determined from the high-resolution A-array map.

galaxy 3C 40 (PKS 0123−016B), and it is identified with the elliptical galaxy NGC 541 in the cluster Abell 194. Our attention was drawn to PKS 0123−016A because low-resolution radio maps at 2.8 cm showed that the source is nearly unpolarized and has the strange, blue "Minkowski's object" (Minkowski 1958; Simkin 1976) located at one end (Andernach 1982). It had been proposed that this object is a peculiar double galaxy (Minkowski 1958), an extragalactic H II region having some of the characteristics of active radio galaxies (Simkin 1976), or even a blob of gas ejected from NGC 541 (Burbidge 1976).

The location of Minkowski's object with respect to PKS 0123−016A suggested to us that the radio and optical emission are morphologically related, perhaps similar to the situation observed in 3C 277.3 (Paper I). Our new radio and optical images substantiate this. Compared to the radio/optical knot in 3C 277.3, however, important differences do exist: Minkowski's object exhibits unusually bright optical continuum emission, and its spectrum resembles those of galaxies dominated by giant H II regions (French 1980). Observations of the prototypical starburst galaxy NGC 7714 (Weedman *et al.* 1981) confirm that the optical emission from Minkowski's object is caused by photoionization of gas by type O and B stars. The extensive starburst was probably triggered by the radio jet emanating from NGC 541.

Some global properties of Minkowski's object, NGC 541, and PKS 0123−106A are given in Table 1. Unless otherwise stated, we assume a Hubble constant of 75 km s^{-1} Mpc^{-1} and $q_0 = 0.5$ throughout this paper.

II. OBSERVATIONS

Radio and optical data were obtained at several observatories, as summarized in Table 2. Standard procedures were followed for their calibration and analysis (see, e.g., Paper I).

a) Radio Imaging

Two sets of radio observations were taken with the Very Large Array (Thompson *et al.* 1980). The first set (A-array) was aimed at obtaining high-resolution information for detailed comparison with our optical CCD images. These data were combined with brief (1 hr total) observations in the lower resolution B- and C-arrays (kindly provided by Dr. C. O'Dea) for better sensitivity to extended radio emission. The complex

TABLE 2

JOURNAL OF OBSERVATIONS

Parameter (1)	Radio Image (2)	Radio Image (3)	Optical Image (4)	Optical Image[a] (5)	Slit Spectrum (6)	Slit Spectrum[b] (7)	Slit Spectrum (8)	Aperture Spectrum (9)
Telescope	VLA	VLA	CTIO 4 m	ESO 1.5 m	KPNO 4 m	Lick 3 m	Lick 3 m	Lick 3 m
Instrument (or configuration)	A-array	C-array	Prime CCD	Cassegrain CCD	cryogenic camera	Cassegrain CCD	Cassegrain CCD	Cassegrain ITS
Angular resolution (or aperture)	3".4 × 2".4 (P.A. 10°)	13" × 13"	1"	1"	2"	2"	2"	4" × 4"
$\Delta\lambda$ band	12.5 MHz @ 1.4 GHz	12.5 MHz @ 1.4 GHz	75 Å on Hα	~115 Å on/off Hα	4500–7900 Å	4800–7500 Å	6000–7200 Å	3240–5360 Å
Spectral resolution	...	...	...	...	15 Å	15 Å	7 Å	5 Å
Position angle	...	...	...	...	57°	129°	129°	0°
Location	...	...	...	...	N 541 + jet	ridge + NW*	ridge + NW*	~SE knot
Time (hr)	2.5	2.5	1.0	2 × 1	0.5	0.5	1.0	2 × 1.5
Date	1983 Sep	1984 Jun	1983 Sep	1983 Nov	1983 Aug	1984 Jul	1984 Aug	1984 Oct
Purpose	radio structure of NGC 541		optical structure of Minkowski's object		kinematics, ionization state		gas ionization mechanism, n_e	

[a] The two narrow-band filters, centered at 6652 Å ($\Delta\lambda$ = 112 Å) and 6573 Å ($\Delta\lambda$ = 120 Å), include and omit (respectively) the Hα + [N II] emission lines at the redshift of Minkowski's object ($z \approx 0.0187$).
[b] Data kindly obtained for us by Dr. H. Spinrad and S. Djorgovski. Slit positioned along the bright "ridge" and through a star to the NW (see Fig. 4).

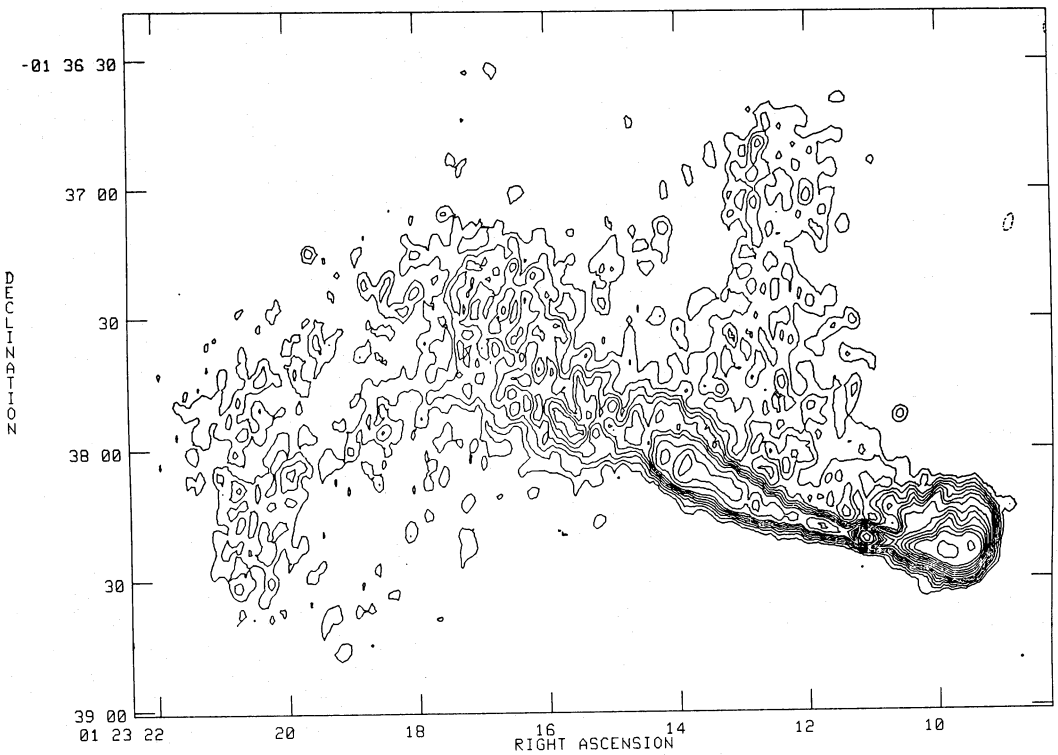

FIG. 1.—Contour representation of the total intensity of PKS 0123−016A, observed at 21 cm with 3.″4 × 2.″4 resolution (P.A. ≈ 10°). Contour values are at levels of −0.4 (*dashed*), 0.4, 0.6, 0.8, 1.0, 1.2, 1.4, 1.6, 1.8, 2.0, 2.2, 2.4, 2.6, 2.8, 3.2, 3.6, 4.0, 4.4, 4.8, 5.2, and 5.6 mJy beam^{-1}. Note the jet to the NE.

visibility data were tapered slightly to obtain a good compromise between high resolution (3.″4 × 2.″4, P.A. = 10°) and sensitivity to extended emission having low surface brightness (Fig. 1).

The second set (C-array) is part of a more complete study of the PKS 0123−016A/B field to obtain multifrequency information on polarization and total intensity. Full analysis of these radio data is deferred to a future paper. The observations presented here are of relatively low resolution (13″ × 13″), and serve only to show the general morphology and polarization structure of PKS 0123−016A (Fig. 2).

b) Optical Imaging

Photometrically calibrated images were obtained with CCDs on the 4 m telescope at Cerro Tololo Inter-American Observatory and on the Danish 1.5 m reflector at the European Southern Observatory. These observations were made through narrow-band filters centered on the {Hα λ6563 + [N II] λλ6548, 6583} emission lines at the redshift of Minkowski's object (Table 1). With the 1.5 m telescope, a corresponding line-free image of the optical continuum was also obtained. Central portions of the CTIO Hα + [N II] image are shown in Figures 3 and 4 (Plates 8 and 9) at two different intensity scales, and the radio contours (Fig. 1) are superposed on the optical image in Figure 5.

The total Hα + [N II] flux is 3.2×10^{-14} ergs s^{-1} cm^{-2} (integrated over a 12″ × 16″ area), half of which originates in a ridge (2.″5 × 8.″5) that includes two bright knots (Figs. 3 and 4). Over the same 12″ × 16″ area, the total flux density at the central wavelength (6573 Å) of the continuum narrow-band filter is 4.0×10^{-16} ergs s^{-1} cm^{-2} Å^{-1}.

c) Long-Slit Spectroscopy

To obtain information on the kinematics, ionization state, and density of the emission-line gas, spectra were obtained through long, narrow slits with the cryogenic camera on the 4 m Mayall telescope at Kitt Peak National Observatory and the new CCD spectrograph (designed by Dr. J. Miller) on the 3 m Shane telescope at Lick Observatory. For the "ridge" in Figure 4, the spectrophotometric Lick data are in excellent agreement with fluxes derived from our images. Lick spectra with 7 Å resolution (full width at half-maximum [FWHM]) allow us to resolve the Hα and [N II] λλ6548, 6583 blend as well as the [S II] λλ6716, 6731 doublet, as shown in Figure 6.

d) Aperture Spectroscopy

The strengths of high-excitation lines (such as He II λ4686 and [Ne V] λ3426) relative to Hβ and [O II] λ3727 provide important discriminants between different ionization models. To this end, and to determine the possible presence of Balmer absorption lines, we observed Minkowski's object using the image-tube scanner (ITS) (Robinson and Wampler 1972) on the Lick 3 m telescope. The object and background sky were recorded simultaneously through a pair of square entrance apertures (4″ × 4″) separated in the N–S direction by 35″, and the beams were switched every 8 minutes. At the chosen orientation, the "sky" apertures allowed approximate removal of the faint outer envelope of NGC 541. We attempted to center the bright SE knot (Fig. 4) on each aperture, but an uncertainty of ∼2″ exists owing to the faintness of the diffuse image on the TV screen used for guiding.

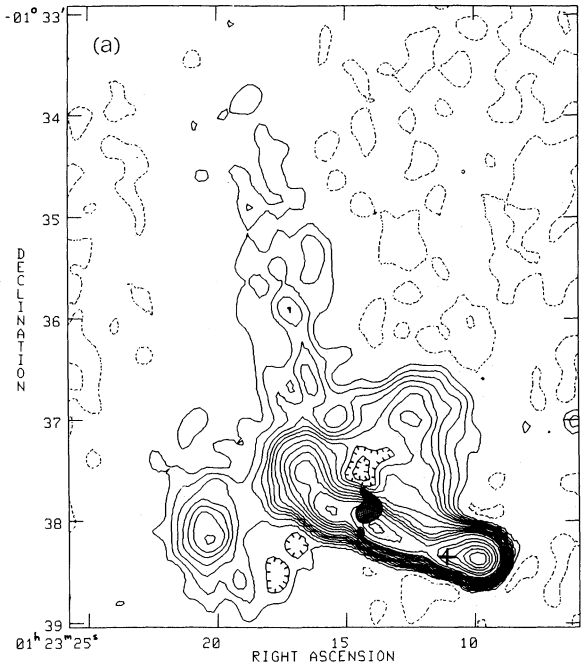

FIG. 2*a*

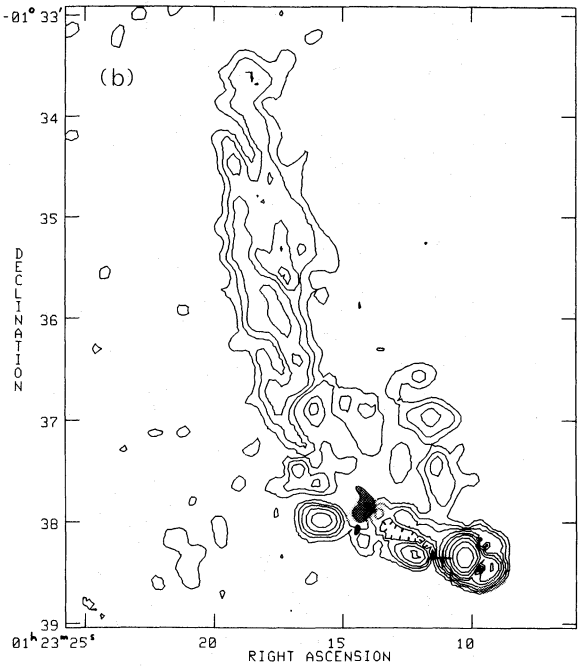

FIG. 2*b*

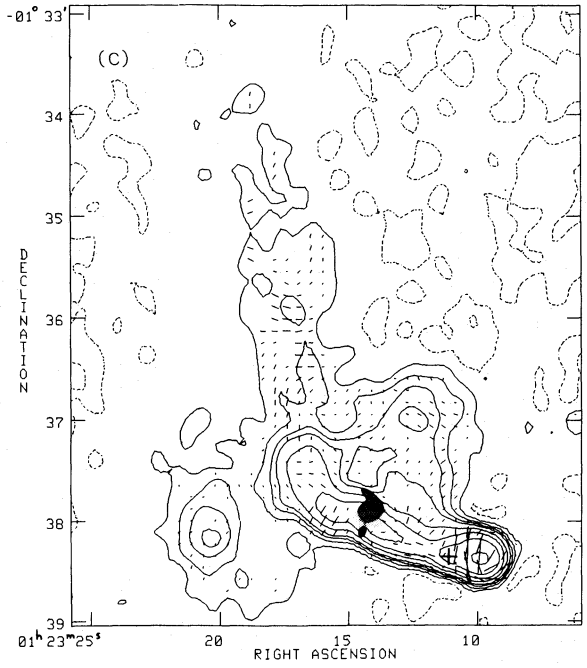

FIG. 2*c*

FIG. 2.—(*a*) Contour representation of the total intensity of PKS 0123−016A, observed at 21 cm with 13″ × 13″ resolution. Contour values are at levels of 0.33 mJy beam^{-1} × (−2, 2, 4, 6, 8, 10, 12, 15, 20, 25, 30, 35, 40, 50, 70, 85, 110, 130, 150). The location of Minkowski's object is indicated by gray shading; the nucleus of NGC 541 is shown by a cross. Note the "wiggles" in the radio jet downstream from Minkowski's object. (*b*) Contour representation of the polarized intensity. Contour values are at levels of 0.13 mJy beam^{-1} × (3, 5, 7, 10, 14, 18, 25, 35, 50). Note the absence of polarized emission in the vicinity of Minkowski's object. (*c*) Contours representing the total intensity at levels of 0.33 mJy beam^{-1} × (−2, 2, 6, 10, 14, 25, 40, 70, 150). Superposed line segments represent the polarization position angles with their lengths proportional to the polarized intensity (at a scale of 1″ corresponding to 0.3 mJy beam^{-1}).

The ITS spectrum of Minkowski's object is shown in Figure 7*a*. Data were smoothed with a 5 Å Gaussian (FWHM) to yield a final resolution of ∼7 Å. Major emission lines are labeled, but most of the undulations in the continuum must be noise. Several particularly prominent features caused by ion events in the detector or by poor subtraction of night-sky lines are marked.

III. RESULTS

a) Radio Maps

The observations by O'Dea and Owen (1984) have already shown that PKS 0123−016A is a small head-tail source associated with NGC 541. Our high-resolution map illustrates more clearly the jet to the NE, as well as a strongly curved, "folded" counterjet to the SW. The NE jet starts at the nucleus, remains fairly straight, and slowly diverges until it reaches the region of optical emission, beyond which it twists in a spiraling fashion and decollimates. Near Minkowski's object the lateral expansion rate of the jet, defined as the ratio of its width to its distance from the nucleus (Bridle 1984), is ∼0.28. Assuming little local and Galactic foreground Faraday rotation (the latter expected from the high Galactic latitude of $b^{II} = -63°$; Simard-Normandin and Kronberg 1979), the polarization distribution (Fig. 2) implies a large-scale magnetic field (***B***) morphology for the jet similar to that of other head-tail sources (e.g., van Breugel 1982); ***B*** is parallel to the jet at the boundaries, and transverse within the jet. When compared to the total and nuclear radio power of PKS 0123−016A (Table 1), all these properties are quite normal for low-luminosity radio sources (see Bridle 1984). They suggest that the jet associated with Minkowski's object is probably of relatively low power.

b) Comparison with the Optical Image

The CTIO narrow-band image is shown in Figure 5, superposed on the high-resolution radio map. The location of Mink-

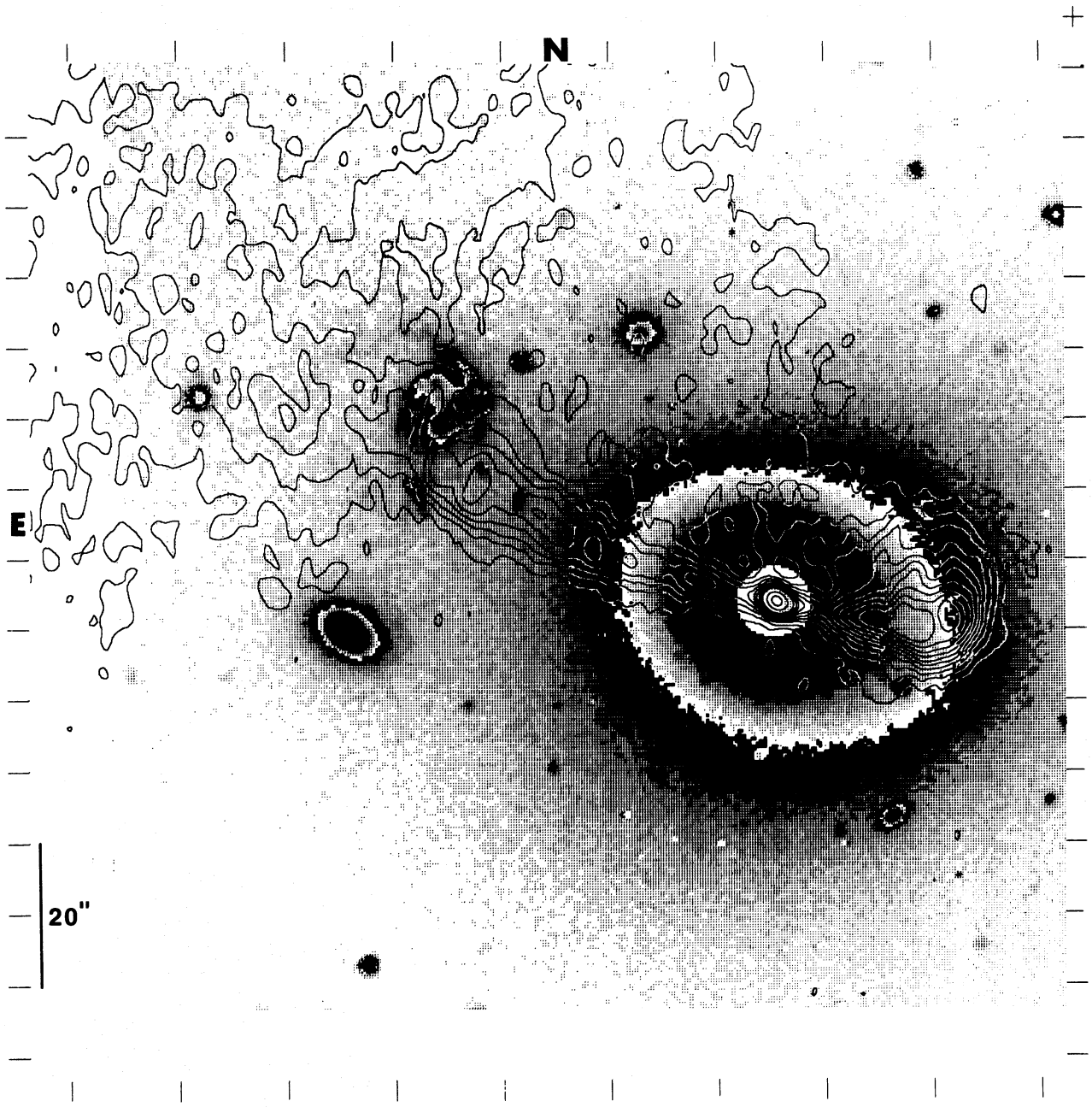

FIG. 5.—Same as Fig. 3, but with radio map (Fig. 1) superposed. Contours represent the total intensity at 21 cm at levels of 0.5, 1, 1,5, 2, 2.5, 3, 3.5, 4, 4.5, 5, 7, and 9 mJy beam^{-1}. Note Minkowski's object at the end and slightly to the side of the NE jet. Some optical emission can also be seen at the opposite side of the jet.

owski's object is also indicated as a gray region in the low-resolution maps (Fig. 2). To align the radio and optical images we assumed exact coincidence of the corresponding nuclei. We note the following:

1. Minkowski's object is located at the end and slightly to the side of the NE radio jet, and some fainter optical emission is found on the opposite side of the jet. The entire region has the overall appearance of a "cap" at the end of the jet.

2. Downstream from the bright optical ridge the radio jet is decollimated and also deflected to some extent.

3. The optical emission has its sharpest intensity gradient at the upstream side of the jet. This "ridge" includes the two bright knots we refer to as "SE" and "NW." Several other, fainter knots and filaments can be seen downstream.

4. At the location of Minkowski's object no radio polarization is observed. The best limits are obtained from 21 cm maps with 4".2 resolution (van Breugel 1985). These show $\lesssim$ 4% polarization at the center of the jet near Minkowski's object. In contrast, the polarization of the jet in the upstream direction is $\gtrsim$9%.

The above properties are similar to those of other radio jets associated with optical emission lines (see § I for references).

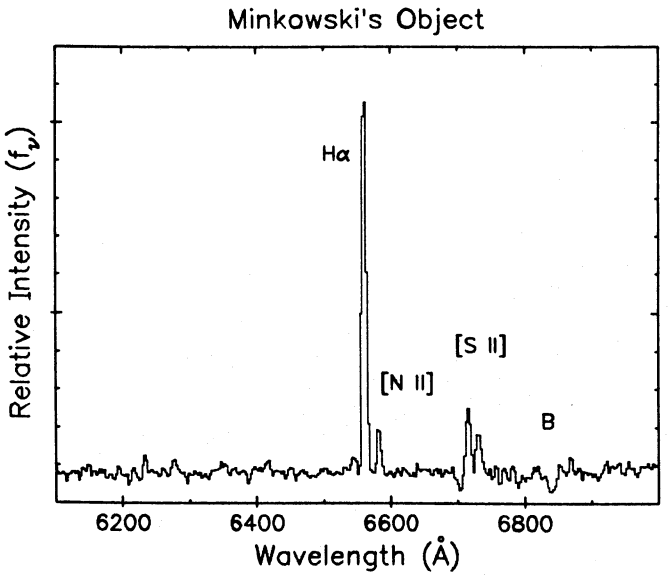

FIG. 6.—Lick CCD spectrum (7 Å resolution) of the NW + SE knots of Minkowski's object. Note the absence of [O I] λ6300 emission. The "absorption" feature immediately to the blue of [S II] λ6716 was caused by a bad column in the CCD. "B" refers to the atmospheric O_2 absorption band.

c) *Spectroscopy*

Relative intensities and equivalent widths of the emission lines are given in Table 3. Although strengths of features in the ITS spectrum were directly compared with that of Hβ, lines to the red of ~5360 Å could only be measured with respect to Hα in the high-resolution (7 Å) Lick CCD data. The low-resolution (15 Å) Lick CCD spectrum, which includes both Hα and Hβ, was subsequently used to determine $F(\mathrm{H}\alpha)/F(\mathrm{H}\beta)$. A value of 3.9 was found, but this is uncertain by ±20% due to inaccuracies in the flux calibration near Hβ and to the different effective apertures used for the CCD and ITS spectra. All red lines are similarly affected when compared with Hβ (but not with Hα).

TABLE 3

OBSERVED RELATIVE INTENSITIES AND EQUIVALENT WIDTHS

	Minkowski's Object[a]		NGC 7714 Nucleus	
Line	$F/F(\mathrm{H}\beta)$	E.W.(Å)	$F/F(\mathrm{H}\beta)$	E.W.(Å)
[Ne V] λ3426	<0.30[b]	<8.6[b]	<0.02	<0.5
[O II] λ3727	2.62	65.9	1.50	58.8
[Ne III] λ3869	0.13	2.4	0.057	1.8
Hγ λ4340	0.38	6.7	0.36	12
[O III] λ4363	≲0.12	<2.2	0.044	1.5
WR λ4640	0.32	5.7	0.095	3.2
He II λ4686	<0.05	<1	0.04	1.3
Hβ λ4861	1.00[c]	18.5	1.00[c]	36.6
[O III] λ4959	0.80	15.5	0.51	18.4
[O III] λ5007	2.29	44.7	1.58	57.4
He I λ5876	<0.09[d]	<2	0.17[e]	...
[O I] λ6300	<0.06[d]	<1.5	0.069[e]	...
[N II] λ6548	0.17[d]	4.1	0.64[e]	...
Hα λ6563	3.9[d]	90	5.04[e]	...
[N II] λ6583	0.45[d]	11	1.85[e]	...
[S II] λ6716	0.60[d]	15	0.49[e]	...
[S II] λ6731	0.46[d]	12	0.51[e]	...

[a] SE knot in ITS spectrum ($\lambda \leq 5360$ Å); SE + NW knots in CCD spectrum ($\lambda > 5360$ Å).

[b] Very crude upper limit due to ion spike in spectrum.

[c] $F(\mathrm{H}\beta)$ through 4″ × 4″ ITS aperture: $\sim 1.3 \times 10^{-15}$ ergs s^{-1} cm^{-2} for Minkowski's object, $\sim 2.6 \times 10^{-13}$ for NGC 7714.

[d] Line measured in same spectrum as Hα, not Hβ. $F(\mathrm{H}\alpha)/F(\mathrm{H}\beta)$ uncertain by about ±20%.

[e] Taken from French 1980.

The Balmer decrement, $F(\mathrm{H}\alpha)/F(\mathrm{H}\beta)/F(\mathrm{H}\gamma) = 3.9/1.0/0.38$, is somewhat steeper than that expected for case B recombination (Brocklehurst 1971), indicating the probable presence of dust in Minkowski's object. Since Hγ may be significantly affected by absorption (see § IV), only Hα and Hβ were used to derive a reddening of $E(B-V) \approx 0.27$ mag. Very little of this

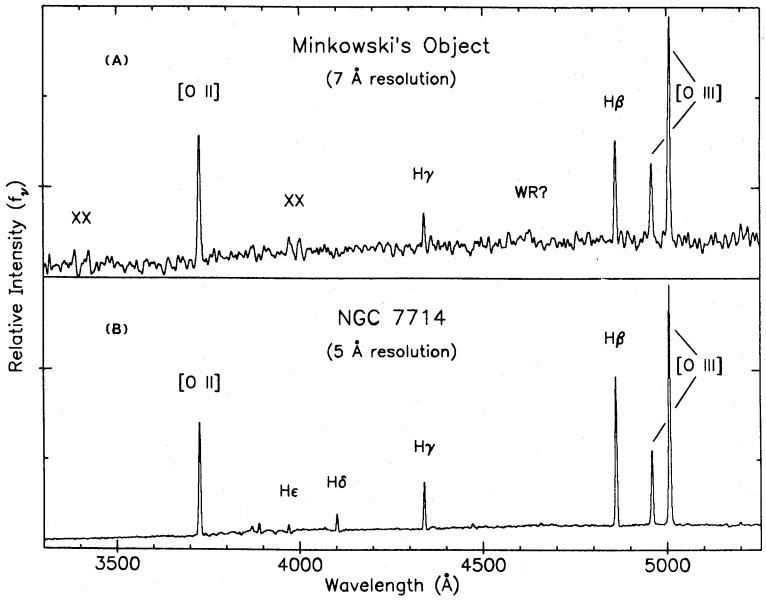

FIG. 7.—Lick ITS spectra of (*a*) Minkowski's object and (*b*) the starburst galaxy NGC 7714, shifted to zero redshift. Only prominent emission lines are marked, although many more are visible in NGC 7714 (as are Balmer absorption lines). "XX" refers to ion events or poor subtraction of the sky. Possible emission due to Wolf-Rayet stars is shown in Minkowski's object. In overall appearance the two spectra are very similar.

($\lesssim$0.02 mag) could have a Galactic origin (Burstein and Heiles 1982). Whitford's (1958) extinction law, as parameterized by Rayo, Peimbert, and Torres-Peimbert (1982), was subsequently used to deredden the emission-line intensity ratios (Table 4).

We measure a value of 1.30 ± 0.1 for I([S II] λ6716)/I([S II] λ6731), implying an average electron density of 180 ± 90 cm^{-3} in the bright knots (Cantó *et al.* 1980). All emission lines are unresolved in both the ITS (5 Å FWHM at Hβ) and CCD (7 Å FWHM at Hα) spectra, implying that the intrinsic width of emission lines is $\lesssim$200 km s^{-1}. Our slit spectra, however, hint that the gas might be kinematically disturbed: the bright NW knot is redshifted by $\sim 100 \pm 70$ km s^{-1} with respect to its nearby ($\sim$2.5 kpc) SE counterpart, and the cryogenic camera observations (Table 2) suggest that the fainter gas a few kpc NE of these knots might be redshifted by 100–200 km s^{-1} relative to the mean of the knot velocities. On the other hand, recent observations with the Lick CCD spectrograph with better spectral resolution ($\sim$7 Å) and at a position angle of 35° through the brightest filament show no large velocity gradient ($\lesssim$120 km s^{-1}) along this direction.

IV. DISCUSSION

At the location of Minkowski's object very little radio polarization is observed (Fig. 2 and § III*b*), suggesting that the ionized gas associated with Minkowski's object is Faraday-depolarizing the radio emission. Moreover, the optical emission exhibits a steep intensity gradient ("ridge") at the end of the well-defined portion of the NE radio jet in PKS 0123−016A (Fig. 5). Beyond (or "downstream" from) this position, the luminous gas is filamentary and may increase somewhat in velocity, while the radio jet is deflected and becomes considerably more diffuse.

These properties are similar to those in other jets associated with optical line emission. They provide evidence for a direct encounter between the radio jet and Minkowski's object. During this encounter the jet entered a region of enhanced gas density, swept a path through it, and entrained clouds of gas in the boundary layers. In particular, this resembles both qualitatively and quantitatively (Table 5) the radio/optical knot (K_1) in 3C 277.3 (Paper I). There are, however, some important differences:

1. The ratio of the optical continuum luminosity (L_o) of Minkowski's object to the total radio luminosity (L_r) of PKS 0123−016A is $\sim$70 times larger than the analogous ratio in 3C 277.3 (Table 5).

2. The radio jet in PKS 0123−016A starts near the nucleus, while the jet in 3C 277.3 is not visible (and hence does not radiate much) until it is near the optical knot, at $\sim$10 kpc from the nucleus. Also, the lateral expansion rate of the jet near Minkowski's object is significantly larger than that in 3C 277.3. This, together with point 1, suggests that the collimated beam in PKS 0123−016A is very dissipative (inefficient) compared to that in 3C 277.3.

3. Most importantly (and perhaps related to the above differences), the spectrum of Minkowski's object is unlike that of knot K_1, as we will now describe.

a) Excitation of the Gas

The main goal of our spectroscopic observations was to determine the nature of the ionization mechanism in Minkowski's object. Simkin (1976) found that the emission-line spectrum resembles those of isolated extragalactic H II regions (Searle and Sargent 1972) in some ways, and the radio galaxies Cyg A and 3C 390.3 in others. Specifically, the possible presence of high-excitation lines such as [Ne V] λ3426 and He II λ4686 suggested activity similar to that in Seyfert galaxies and QSOs. This is particularly intriguing because the nonstellar

TABLE 4

COMPARISON OF DEREDDENED RELATIVE INTENSITIES, $I(\lambda)/I(\mathrm{H}\beta)$

Line (1)	Minkowski's Object (2)	N 7714 (3)	H II (4)	Liner (5)	Shock (6)	Power 1 (7)	Power 2 (8)
[O II] λ3727	3.47	2.50	3.37	5.0	5.2	6.4	1.6
[Ne III] λ3869	0.17	0.089	0.21	0.28[a]	...	0.9[b]	...
[O III] λ4363	$\lesssim$0.13	0.055	...[c]	$\lesssim$0.06	0.10	0.025	0.10
He II λ4686	<0.05	0.04	...[c]	$\lesssim$0.08	0.04	0.17	0.23
Hβ λ4861	1.00	1.00	1.00	1.00	1.00	1.00	1.00
[O III] λ5007	2.23	1.50	2.34	1.43	2.26	2.18	4.0
He I λ5876	<0.08[d]	0.12[e]	0.11	0.11	0.16	0.18	0.16
[O I] λ6300	<0.05[d]	0.042[e]	0.065	0.8	1.0	0.96	0.26
Hα λ6563	2.87[d]	2.87[e]	2.87	2.8	3.1	3.1	3.1
[N II] λ6583	0.33[d]	1.05[e]	0.67	3.3	1.4	1.6	0.40
[S II] λ6716	0.43[d]	0.27[e]	0.37	1.0	2.7	1.1	0.39
[S II] λ6731	0.33[d]	0.28[e]	0.24	1.3	2.1	1.4	0.47

Col. (1).—Line identification.
Col. (2).—Minkowski's object, dereddened using $E(B-V) = 0.27$ (from Hα/Hβ).
Col. (3).—NGC 7714 nucleus, dereddened using $E(B-V) = 0.49$ (from Hα/Hβ).
Col. (4).—Average of Mrk 109, Mrk 168, and NGC 3690 from French 1980. $\langle$O/H$\rangle \approx 2.6 \times 10^{-4}$.
Col. (5).—Mean "Liner" spectrum, from Table 3 of Ferland and Netzer 1983 (FN83).
Col. (6).—Shock model J, from Shull and McKee 1979. v(shock) = 100 km s^{-1}, n(preshock) = 10 cm^{-3}, "depleted" metal abundances.
Col. (7).—"Liner" power-law photoionization model (FN83). log $U = -3.5, \alpha = 1.5$, 0.3 solar abundances.
Col. (8).—Power-law photoionization model (FN83). log $U = -3, \alpha = 1.5$, 0.1 solar abundances.
[a] From Fig. 1 of Halpern and Steiner 1983.
[b] From p. 177 of Halpern 1982.
[c] Line extremely weak (as in other H II regions); not measured.
[d] Line measured in same spectrum as Hα, not Hβ. I(Hα)/I(Hβ) uncertain $\approx \pm 20\%$.
[e] Taken from French 1980.

TABLE 5

COMPARISON OF MINKOWSKI'S OBJECT AND THE RADIO/OPTICAL JET IN 3C 277.3

Parameter	Minkowski's Object in PKS 0123−016A	Knot K_1 in 3C 277.3[a]	Notes
Distance from nucleus (kpc)	18	10	1
Size (kpc^2)	4.5 × 5.5	2.5 × 2.5	1
Radio luminosity (ergs s^{-1})	4×10^{39}	4×10^{40}	2
Emission-line luminosity (ergs s^{-1})	7×10^{41}	7×10^{42}	3
Optical continuum luminosity (ergs s^{-1})	1.5×10^{42}	2×10^{42}	4
Jet expansion rate	0.28	<0.1	5
Average gas density (cm^{-3})	180	300	6
Mass of ionized hydrogen ($M_\odot$)	6×10^5	2×10^6	7
Volume filling factor	4×10^{-6}	1×10^{-5}	8

NOTES.—(1) $H_0 = 75$ km s^{-1} Mpc^{-1}, $q_0 = 0.5$. (2) Taken from 10^7–10^{11} Hz and adopting standard assumptions (Paper I). The corresponding luminosities of PKS 0123−016A and 3C 277.3 are 7.8×10^{40} (using spectral index 0.9; Andernach 1981) and 6.7×10^{42}, respectively. (3) Corrected for extinction, and assuming case B recombination. We estimate that the total emission-line luminosity in Minkowski's object is ~20 times Hα at *all* positions. (4) Defined as frequency multiplied by monochromatic flux density (νf_ν). (5) Defined as the ratio of jet width to distance from the nucleus. Measured at the location of the optical emission. (6) Derived from the observed I([S II] λ6716)/I([S II] λ6731) ratio (Cantó *et al.* 1980). (7) Case B recombination and $T_e \approx 10^4$ K assumed (Osterbrock 1974). (8) Derived from the "actual" line-emitting volume and the "observed" volume. Thickness 1 kpc assumed in Minkowski's object; spherical symmetry in K_1.

[a] For parameters of 3C 277.3, see Paper I.

ionizing radiation could be provided by the newly discovered radio jet from NGC 541. By analogy to the jet and knot in 3C 277.3, the existence of such high-ionization emission lines might indeed be expected.

Inspection of Figure 7*a* and Table 4, however, shows that He II λ4686, [Ne V] λ3426, and even [Ne III] λ3869 are weak or absent, eliminating the possibility of a strong ionizing continuum at high energies. This does not agree with Simkin's (1976) measurements, but the old spectra were recorded on photographic plates and are relatively noisy. Hence, the ionization parameter (U) cannot be greater than $\sim 10^{-3}$ (Ferland and Netzer 1983). As shown in column (8) of Table 4, a satisfactory fit is not achieved if $U = 10^{-3}$ even under the assumption of very low metal abundances (0.1 solar); He II λ4686 and [O I] λ6300 remain particularly discrepant.

At first glance, the comparable strengths of [O II] λ3727 and [O III] λ5007 suggest that Minkowski's object may resemble a "low-ionization nuclear emission-line region" ("Liner") (Heckman 1980). Although gas in Liners was originally thought to be heated by shocks, recent theoretical and observational studies (Ferland and Netzer 1983; Halpern and Steiner 1983; Filippenko and Halpern 1984; Filippenko 1985) indicate that photoionization by a very dilute nonstellar continuum is probably the dominant excitation mechanism. In this case Minkowski's object could indeed be ionized by radiation from the radio jet, as is knot K_1 in 3C 277.3, but the ionization parameter would be small ($U < 10^{-3.5}$). Comparison with the average Liner spectrum in column (5) of Table 4, however, shows that [O I] λ6300, [N II] λ6583, and other low-ionization lines are much too weak in Minkowski's object. Predictions of both shock (col. [6]) and power-law photoionization models with low U (col. [7]) are also inconsistent with these observations.

The last plausible alternative, and one that was discussed by Simkin (1976), is that Minkowski's object may be an enormous H II region in which radiation from hot young stars photoionizes the gas. All of the major emission-line intensity ratios used in the two-dimensional classification schemes of Baldwin, Phillips, and Terlevich (1981) lead to this conclusion. Moreover, comparison with NGC 7714 (Fig. 7*b*), a prototypical "starburst" galaxy (Weedman *et al.* 1981) whose spectrum was also recorded with the Lick ITS, reveals a strong resemblance to Minkowski's object. Tables 3 and 4 show that the relative intensities and equivalent widths of important diagnostic lines such as He II λ4686 and [O I] λ6300 are similar in both galaxies, and there can be little doubt that Minkowski's object is experiencing a burst of star formation. Small discrepancies between the strengths of [O II], [O III], and a few other lines can easily be explained by differences in the abundances. Only the relative intensity of [N II] λ6583 is substantially different in the two galaxies, but this line can once again be adjusted by changing the abundances. In fact, the N abundance of NGC 7714 is known to be quite high relative to that of O (French 1980).

In NGC 7714, prominent Balmer absorption lines underneath the corresponding emission provide direct evidence for the presence of young, massive stars. The signal-to-noise ratio in the spectrum of Minkowski's object is not sufficiently high to allow unambiguous detection of similar features, but there is a hint of absorption beneath the weak Hδ emission (Fig. 7*a*). The steep Balmer decrement (Table 3) is probably caused at least partially by the underlying absorption, so Hγ was not used to determine the reddening (§ III*c*).

Close inspection of Figure 7*a* reveals that broad emission normally associated with Wolf-Rayet stars may exist in Minkowski's object at ~4640 Å (see, e.g., D'Odorico, Rosa, and Wampler 1983). Since such stars are massive and very young, they strongly suggest that vigorous star formation occurred recently. They are known to exist in several other giant extragalactic H II regions (e.g., Kunth and Sargent 1981; Osterbrock and Cohen 1982). Wolf-Rayet features are also present in the spectra of NGC 7714, but at a much weaker level relative to Hβ than in Minkowski's object. Kunth and Joubert (1985) find considerable scatter in the relative strengths of Hβ and Wolf-Rayet lines in a large sample of galaxies, so the difference between our two objects is not unusual.

b) The Continuum

The continua of Minkowski's object and NGC 7714 are similar (Fig. 7). As mentioned by Simkin (1976), Minkowski's object is very blue, implying a population of hot young stars. There is a noticeable decrease in the flux density at wavelengths shorter than $\sim$3750 Å, just like in NGC 7714. This spectral break is probably due to the blending of high-order Balmer absorption lines, which are known to exist in hot stars. It is possible, however, that a portion of the change in slope may be indicative of absorption features in old stars. The blue continuum ($U-B = -0.55 \pm 0.25$; Simkin 1976) and equivalent width of the Hβ emission line (Table 3) in Minkowski's object are consistent with models of starbursts in galaxies which also contain some old stars (Huchra 1977). Better spectra are clearly necessary to quantify the contribution of an old (preexisting?) stellar population in Minkowski's object.

c) Origin of the Gas

In Paper I we argued that the relatively weak [N II] λ6583 line in the optical knot (K_1) of 3C 277.3 demonstrates that the line-emitting gas is probably metal poor. This is consistent with power-law photoionization models which seem to best match the optical spectrum of the knot. A similar conclusion was reached by Simkin, Bicknell, and Bosma (1984) for the optical knot in NGC 7385. Thus, the line-emitting gas in these objects is most likely of local origin, rather than nuclear ejecta which would be expected to have at least solar metallicity (see Pagel and Edmunds 1981). Perhaps the origin of gas in Minkowski's object can be deduced in a similar manner.

The spectral characteristics of H II regions are quite sensitive to the electron temperature (T_e) of the gas. Careful analysis of the metal abundances therefore requires accurate knowledge of T_e, which in principle may be estimated if the [O III] λ4363 emission line can be accurately measured. Unfortunately, our data are too noisy to be of value in this respect. A rough estimate of the O/H ratio, however, can be made by comparison with the results of Kunth and Sargent (1983) and French (1980). The emission-line intensity ratios show that metals are not as deficient as in typical isolated extragalactic H II regions, but they nevertheless have subsolar abundances. Particularly good agreement was found by averaging the data for Mrk 109, Mrk 168, and NGC 3690 from French (1980), as can be seen in columns (2) and (4) of Table 4. These galaxies have O/H abundance ratios of 2.7, 2.6, and 2.4 (respectively) in units of 10^{-4}, whereas the "cosmic" value is 6.8 (Kunth and Sargent 1983). Most of the relative strengths agree to within 20%, with only [N II] λ6583 seriously different ($\sim$100%).

It therefore appears as though Minkowski's object is especially deficient in nitrogen. Since all three of the French (1980) galaxies are very luminous while Minkowski's object has $M_B \approx -17.5$ (Simkin 1976), this may support the conclusion of Rubin, Ford, and Whitmore (1984) that the enhancement of N due to secondary nucleosynthetic processing in successive generations of stars is greater in the disks of massive spirals than in low-mass systems. Indeed, the observed intensity ratio of [N II] $\lambda\lambda$6548 + 6583 to [S II] $\lambda\lambda$6716 + 6731 in Minkowski's object is quite normal for its absolute magnitude (Rubin, Ford, and Whitmore 1984). On the other hand, it is possible that the majority of the heavy elements in Minkowski's object were instead produced while the cluster of galaxies was forming; X-ray data for other clusters indicate that halo gas usually has Fe abundances within a factor of 2 of solar (Rothenflug *et al.* 1984).

The location of Minkowski's object in the optical "bridge" which joins NGC 541 and NGC 545/547 suggests that it may also be composed of debris related to the apparent gravitational interaction occurring in this system of galaxies. Galaxy interactions are implicated in several other cases of emission-line gas associated with radio jets and lobes, such as 3C 305 (Heckman *et al.* 1982), 3C 293 (van Breugel *et al.* 1984), 4C 29.30 (van Breugel *et al.* 1985*b*), PKS 0349−278 (Danziger *et al.* 1984), and Cen A (Graham 1979). The exact origin of gas in Minkowski's object, however, is obviously not well understood.

d) Parameters of the Starburst

It is of interest to estimate the number of stars required to ionize the gas in Minkowski's object. The narrow-band CCD images, combined with our spectra, yield an Hα intensity of $\sim 5.0 \times 10^{-14}$ ergs s^{-1} (corrected for extinction using $E[B-V] = 0.27$), so the total Hα luminosity is $\sim 3.4 \times 10^{40}$ ergs s^{-1}. If the gas is optically thin in the Balmer lines and collisional ionization is negligible, this requires the production of $\sim 2.4 \times 10^{52}$ ionizing photons s^{-1} by hot stars. Referring to Table 2.3 in Osterbrock (1974), we find that $\sim 5.1 \times 10^2$ O5 stars, 3.5×10^3 O7 stars, or 1.4×10^4 O9 stars are necessary. Of course, a range of types is undoubtedly involved, so the above analysis is very crude. Following Weedman *et al.* (1981), a more realistic estimate of the total mass can be made simply by scaling the models of Rieke *et al.* (1980); the result is $\sim 1.2 \times 10^7\ M_\odot$. This is more than a factor of 10 smaller than the corresponding mass in NGC 7714, and it implies a supernova rate of only $\sim$0.04 yr^{-1}. Careful monitoring of Minkowski's object could reveal a supernova within a few decades.

The explosion of massive stars in Minkowski's object would result in X-ray and radio emission from supernova remnants (SNRs). Using the *Einstein* X-ray satellite, Jones and Forman (1984) detected several regions with enhanced X-ray emission in the center of Abell 194. One of these X-ray "clumps," with a total luminosity of $\sim 7 \times 10^{40}$ ergs s^{-1} in the 0.5–3.0 keV band, is displaced by $\sim 50'' \pm 30''$ from NGC 541 and lies in the vicinity of Minkowski's object. Could this emission be associated with Minkowski's object itself?

Fabbiano and Panagia (1983) measured the X-ray emission of several extragalactic H II regions and found that $\log (f_X/f_B) < -5$ in all cases. An analogous calculation yields $\log (f_X/f_B) = -2.4$ (in the units of Fabbiano and Panagia) if the X-ray emission noted by Jones and Forman (1984) is related to Minkowski's object, making the latter overluminous in X-rays by at least three orders of magnitude. Furthermore, it would then have approximately the same X-ray luminosity as NGC 7714 and would require a truly prodigious number (10^4–10^5) of SNRs (Weedman *et al.* 1981). This is even more than our previous rough estimate of the number of massive stars involved in the starburst. We therefore next consider whether the X-ray emission may instead be associated with NGC 541.

From an X-ray survey of 3CR radio galaxies, Fabbiano *et al.* (1984) found that the X-ray emission from low-power radio galaxies (FR class I; Fanaroff and Riley 1974) is related to their optical luminosity as well as to the total and nuclear radio power. Using the data in Table 1 for NGC 541, and adopting the units of Fabbiano *et al.* (1984), we calculate that one would expect to see X-rays from NGC 541 at about the observed level; $\log (f_X/f_V) = -6.5$ (where f_V is the flux density at visual

wavelengths) is typical even of radio-quiet ellipticals (see their Fig. 3). Similar results are found from a consideration of the X-ray luminosity and the radio power of the nucleus (Fig. 5 in Fabbiano *et al.*). We conclude that the X-ray emission is probably associated with NGC 541, and cannot be used to derive the number of SNRs in Minkowski's Object.

Another constraint on the number of SNRs can in principle be obtained from the nonthermal radio emission. The total flux density at 21 cm, summed over the angular extent of Minkowski's object, is ~ 30 mJy. This is an upper limit because of the very likely confusion by nonthermal emission from the jet. (The contribution of thermal emission by the H II regions, on the other hand, is estimated from the total Hα luminosity to be < 0.06 mJy.) Following the discussion in Weedman *et al.* (1981) for NGC 7714, we then calculate a rather crude upper limit of 5×10^4 for the number of SNRs in Minkowski's object. Thus, neither the X-ray nor the radio emission provide very tight constraints on the number of SNRs associated with the starburst. Compared with NGC 7714, the starburst in Minkowski's object is relatively modest.

e) Jet-induced Star Formation

Using standard minimum-energy arguments (e.g., Miley 1983), we derive a pressure of $P_r/k \approx 1.2 \times 10^5$ K cm^{-3} for the radio-emitting plasma in Minkowski's object. This is very likely much larger than that of preexisting cool clouds; for comparison, H I clouds in our Galaxy typically have $P_r/k \approx 10^3$ K cm^{-3} (Spitzer 1978). Together with the ram pressure of the jet fluid, this pressure would therefore have a significant impact on clouds in Minkowski's object and on star formation.

The filamentary structure and possibly disturbed kinematics of the ionized gas in Minkowski's object suggest that, prior to their collapse and the ensuing starburst, some of the clouds were entrained by the fluid in the jet boundary layers. Hot, massive stars subsequently formed and photoionized the adjacent comoving gas. The mass of ionized hydrogen is $\sim 6 \times 10^5$ $M_\odot$ (Table 5), far less than that trapped in stars ($\lesssim 1 \times 10^7$ $M_\odot$), and it occupies only a small fraction ($\sim 4 \times 10^{-6}$) of the volume.

The pressure in the ionized gas is $P_g/k = 2n_e T_e \approx 3.6 \times 10^6$ K cm^{-3} since $T_e \approx 10^4$ K in H II regions. This is more than an order of magnitude greater than that of the radio-emitting plasma; hence, the H II regions can easily expand (as they often do in our own Galaxy). If instead they are confined, it must be by the ram pressure (ρv^2) of the jet fluid. This would require $\rho v^2 = 2n_e kT_e$, or $v \approx 170 n_j^{-1/2}$ km s^{-1} in the boundary layers of the jet. (Here ρ, v, and n_j are the mass density, velocity, and thermal electron density of gas in the jet, respectively.) The jet gas density is not known, but in light of the presence of polarized radio emission upstream from Minkowski's object (§ III*b*) we assume that it cannot be large (at least not prior to the collision of the jet with Minkowski's object). If one adopts the "best guess" of $n_j \approx 10^{-2}$ cm^{-3} derived for the Cen A jet by Burns, Feigelson, and Schreier (1983), a velocity of a few thousand kilometers per second is found for the jet in PKS 0123−016A. This value would likely be much higher in the center of the jet.

V. CONCLUSIONS

Our most important conclusion is that radio jets appear capable of stimulating considerable star formation along their trajectories if conditions are favorable. This was already recognized as a possible consequence of jets from the presence of blue objects and H II regions in the outer jet of Cen A and in NGC 7385. It seems, however, that the jet in PKS 0123−016A really hit the "jackpot" by triggering a large burst of star formation in the galactic bridge between its parent galaxy and that of its more powerful neighbor 3C 40. Further spectroscopic observations of Minkowski's object are required to investigate the possible presence of an older population of stars.

The difference in excitation mechanism between the optical/radio knot (K_1) in 3C 277.3 (power-law photoionization) and Minkowski's object (photoionization by OB stars) may be related to differences in the jets that are (indirectly) powering them. The relatively low luminosity and complex radio morphology of PKS 0123−016A suggest a weaker and less collimated jet than in 3C 277.3. We note that Cen A and NGC 7385 also have relatively low radio luminosities. Intuitively, one might expect that star formation cannot occur unless the jet momentum is small, since otherwise the clouds are completely disrupted.

This investigation raises the interesting question of the general importance of jet-induced starbursts. The obvious prerequisite of a jet with a dense ambient medium makes the class of steep-spectrum radio sources having ~ 1 kpc sizes a good hunting ground for the future Space Telescope. Indeed, several members of this class are already known to exhibit clear evidence for the presence of young stars in their parent galaxies; 3C 305 (Heckman *et al.* 1982), 3C 48 (Boroson and Oke 1982), and 3C 459 (Miller 1981; Ulvestad 1984), for example, all exhibit prominent Balmer absorption lines.

We acknowledge stimulating discussions with Drs. C. McKee, C. Norman, S. Simkin, and several other colleagues during the Workshop on Active Galaxies and QSOs at U. C. Santa Cruz (1984 July). It is a pleasure to thank Dr. H. Spinrad and S. Djorgovski for obtaining and calibrating a slit spectrum of Minkowski's object at Lick Observatory, as well as Dr. C. O'Dea for letting us use his VLA data. Many assistants provided excellent support at CTIO, ESO, KPNO, Lick, and the VLA. We also thank the various directors for generous allocations of observing time.

The research of W. v. B. is supported by NSF grant AST 81-14717. A. V. F. is grateful to the Miller Institute for Basic Research in Science for a postdoctoral fellowship. T. H. thanks the Alfred P. Sloan Foundation and the National Science Foundation, the latter for financial support under grant AST 82-16553.

The Very Large Array is a facility of the National Radio Astronomy Observatory, which is operated by Associated Universities, Inc., under contract with the National Science Foundation. Kitt Peak National Observatory and Cerro Tololo Inter-American Observatory are facilities of the National Optical Astronomy Observatories, which is operated by the Association of Universities for Research in Astronomy under contract with the NSF.

REFERENCES

Andernach, H. 1981, Ph.D. thesis, Ruhr-University Bochum, Germany.
———. 1982, in *IAU Symposium 97, Extragalactic Radio Sources*, ed. D. S. Heeschen and C. M. Wade (Dordrecht: Reidel), p. 41.
Baldwin, J. A., Phillips, M. M., and Terlevich, R. 1981, *Pub. A.S.P.*, **93**, 5.
Blanco, V. M., Graham, J. A., Lasker, B. M., and Osmer, P. 1975, *Ap. J. (Letters)*, **198**, L63.
Boroson, T. A., and Oke, J. B. 1982, *Nature*, **296**, 397.
Bridle, A. H. 1984, *A.J.*, **89**, 979.
Brocklehurst, M. 1971, *M.N.R.A.S.*, **153**, 471.
Brodie, J., Königl, A., and Bowyer, S. 1983, *Ap. J.*, **273**, 154.
Burbidge, G. R. 1976, in *The Physics of Nonthermal Radio Sources*, ed. G. Setti (Dordrecht: Reidel), p. 126.
Burstein, D., and Heiles, C. 1982, *A.J.*, **87**, 1165.
Burns, J. O., Feigelson, E. D., and Schreier, E. J. 1983, *Ap. J.*, **273**, 128.
Cantó, J., Elliot, K. H., Meaburn, J., and Theokas, A. C. 1980, *M.N.R.A.S.*, **193**, 911.
Danziger, I. J., Fosbury, R. A. E., Goss, W. M., Bland, J., and Boksenberg, A. 1984, *M.N.R.A.S.*, **208**, 589.
De Young, D. S. 1981, *Nature*, **293**, 43.
———. 1984, *Proc. Greenbank Workshop on Jets*, ed. A. H. Bridle and J. Eilek (Charlottesville: NRAO), in press.
D'Odorico, S., Rosa, M., and Wampler, E. J. 1983, *Astr. Ap. Suppl.*, **53**, 97.
Fabbiano, G., Miller, L., Trinchieri, G., Longair, M., and Elvis, M. 1984, *Ap. J.*, **277**, 115.
Fabbiano, G., and Panagia, N., 1983, *Ap. J.*, **266**, 568.
Fanaroff, B. L., and Riley, J. M. 1974, *M.N.R.A.S.*, **167**, 31P.
Ferland, G. J., and Netzer, H. 1983, *Ap. J.*, **264**, 105.
Filippenko, A. V. 1985, *Ap. J.*, **289**, 475.
Filippenko, A. V., and Halpern, J. P. 1984, *Ap. J.*, **285**, 458.
French, H. B. 1980, *Ap. J.*, **240**, 41.
Graham, J. A. 1979, *Ap. J.*, **232**, 60.
Graham, J. A., and Price, R. M. 1981, *Ap. J.*, **247**, 813.
Halpern, J. P. 1982, Ph.D. thesis, Harvard University.
Halpern, J. P., and Steiner, J. E. 1983, *Ap. J. (Letters)*, **269**, L37.
Hardee, P. E., Eilek, J. A., and Owen, F. N. 1980, *Ap. J.*, **242**, 502.
Heckman, T. M. 1980, *Astr. Ap.*, **87**, 152.
Heckman, T. M., Miley, G. K., Balick, B., van Breugel, W. J. M., and Butcher, H. R. 1982, *Ap. J.*, **262**, 529.
Heckman, T. M., van Breugel, W. J. M., and Miley, G. K. 1984, *Ap. J.*, **286**, 509.
Huchra, J. P. 1977, *Ap. J.*, **217**, 928.
Jones, C., and Forman, W. 1984, preprint.
Kunth, D., and Joubert, M. 1985, *Astr. Ap.*, in press.
Kunth, D., and Sargent, W. L. W. 1981, *Astr. Ap.*, **101**, L5.
———. 1983, *Ap. J.*, **273**, 81.
Miley, G. K. 1983, *Ann. Rev. Astr. Ap.*, **18**, 165.
Miley, G. K., Heckman, T. M., Butcher, H. R., and van Breugel, W. J. M. 1981, *Ap. J. (Letters)*, **247**, L5.
Miller, J. S. 1981, *Pub. A.S.P.*, **93**, 681.
Minkowski, R. 1958, *Pub. A.S.P.*, **70**, 143.
Norman, C. 1984, private communication.
Norman, M. L., Smarr, L., Winkler, K.-H. A., and Smith, M. D. 1982, *Astr. Ap.*, **113**, 285.
O'Dea, C. P., and Owen, F. N. 1984, *A.J.*, in press.
Osmer, P. S. 1978, *Ap. J. (Letters)*, **226**, L79.
Osterbrock, D. E. 1974, *Astrophysics of Gaseous Nebulae* (San Francisco: Freeman).
Osterbrock, D. E., and Cohen, R. D. 1982, *Ap. J.*, **261**, 64.
Pagel, B. E. J., and Edmunds, M. G. 1981, *Ann. Rev. Astr. Ap.*, **19**, 77.
Phillips, M. M. 1981, *M.N.R.A.S.*, **197**, 659.
Rayo, J. F., Peimbert, M., and Torres-Peimbert, S. 1982, *Ap. J.*, **255**, 1.
Rieke, G. H., Lebovsky, M. J., Thompson, R. I., Low, F. J., and Tokunaga, A. T. 1980, *Ap. J.*, **238**, 24.
Robinson, L. B., and Wampler, E. J. 1972, *Pub. A.S.P.*, **84**, 161.
Rothenflug, R., Vigroux, L., Mushotzky, R. F., and Holt, S. S. 1984, *Ap. J.*, **279**, 53.
Rubin, V. C., Ford, W. K., and Whitmore, B. C. 1984, *Ap. J. (Letters)*, **281**, L21.
Searle, L., and Sargent, W. L. W. 1972, *Ap. J.*, **173**, 25.
Shull, J. M., and McKee, C. F. 1979, *Ap. J.*, **227**, 131.
Simard-Normandin, M., and Kronberg, P. P. 1979, *Nature*, **279**, 115.
Simkin, S. M. 1976, *Ap. J.*, **204**, 251.
Simkin, S. M., Bicknell, G. V., and Bosma, A. 1984, *Ap. J.*, **277**, 513.
Spitzer, L. 1978, *Physical Processes in the Interstellar Medium* (New York: Wiley).
Thompson, A. R., Clark, B. G., Wade, C. M., and Napier, P. J. 1980, *Ap. J. Suppl.*, **44**, 151.
Tonry, J. L., and Davis, M. 1981, *Ap. J.*, **246**, 666.
Ulvestad, J. 1984, *Ap. J.*, **288**, 514.
van Breugel, W. J. M. 1982, *Astr. Ap.*, **110**, 225.
———. 1985, private communication.
van Breugel, W. J. M., Heckman, T. M., Butcher, H. R., and Miley, G. K. 1984, *Ap. J.*, **277**, 82.
van Breugel, W. J. M., Heckman, T. M., and Miley, G. K. 1984, *Ap. J.*, **276**, 79.
van Breugel, W. J. M., Heckman, T. M., Miley, G. K., and Filippenko, A. V. 1985*b*, in preparation.
van Breugel, W. J. M., Miley, G. K., Heckman, T. M., Butcher, H. R., and Bridle, A. H. 1985*a*, *Ap. J.*, **290**, 496 (Paper I).
Weedman, D. W., Feldman, F. R., Balzano, V. A., Ramsey, L. W., Sramek, R. A., and Wu, C.-C. 1981, *Ap. J.*, **248**, 105.
Whitford, A. E. 1958, *A.J.*, **63**, 201.
Woodward, P. R. 1984, in *Astrophysical Radiation Hydrodynamics*, ed. K.-H. A. Winkler and M. L. Norman (Dordrecht: Reidel), in press.

ALEXEI V. FILIPPENKO: Department of Astronomy, University of California, Berkeley, CA 94720

TIMOTHY M. HECKMAN: Department of Physics and Astronomy, Johns Hopkins University, Baltimore, MD 21218

GEORGE K. MILEY: Space Telescope Science Institute, Homewood Campus, Baltimore, MD 21218

WIL J. M. VAN BREUGEL: University of California, Radio Astronomy Laboratory, 601 Campbell Hall, Berkeley, CA 94720

PLATE 8

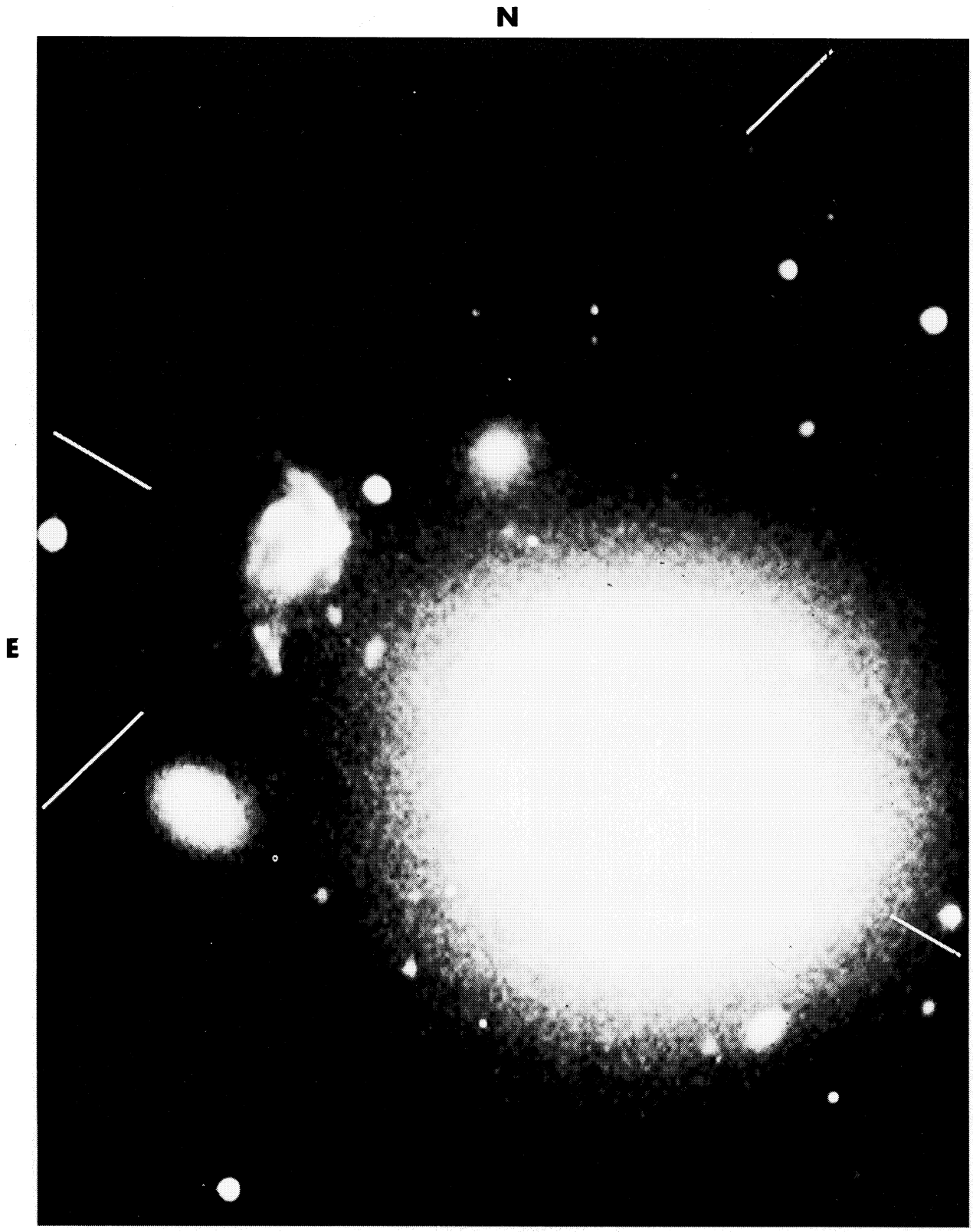

FIG. 3.—Photographic representation of the CTIO image (seeing ~1″) of Minkowski's object and the elliptical galaxy NGC 541. A filter was used to isolate the Hα and [N II] emission lines, but the underlying continuum has not been subtracted. The two slit position angles used in the spectroscopic observations are indicated.

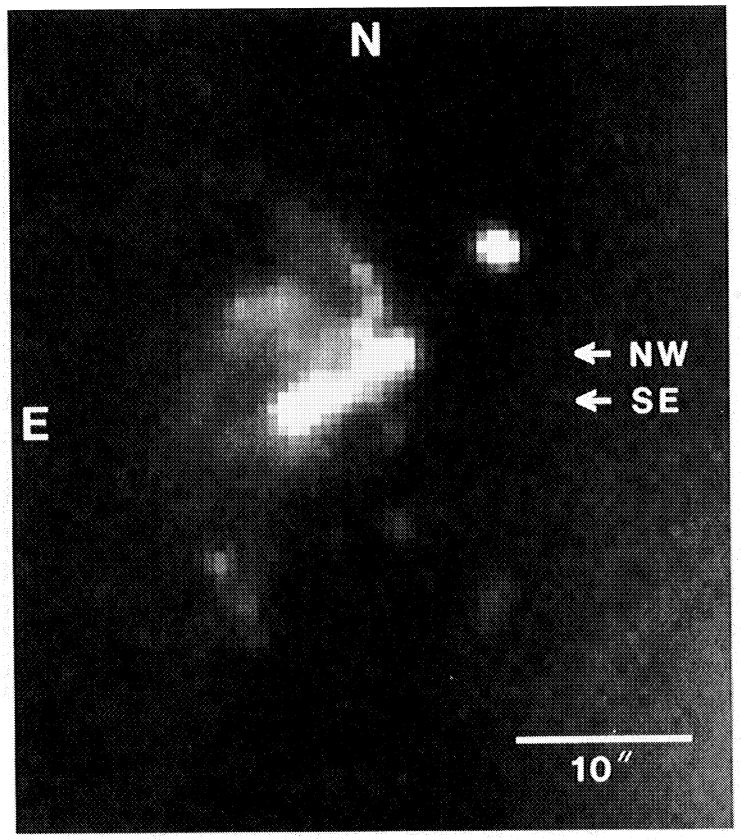

FIG. 4.—A portion of the CTIO Hα + [N II] image (Fig. 3) of Minkowski's object is shown at an intensity level that emphasizes the two compact "knots" called NW and SE, the "ridge" between them, and nearby filaments. Faint light from the outer isophotes of NGC 541 is visible in the SW corner of the photograph.

VAN BREUGAL *et al.* (*see* page 85)